Dynamic Variations at the Base of the Solar Convection Zone

***R. Howe*[1], *J. Christensen-Dalsgaard*[2], *F. Hill*[1], *R.W. Komm*[1], *R.M. Larsen*[3], *J. Schou*[3], *M.J. Thompson*[4], *J. Toomre*[5]**

[1] National Solar Observatory, National Optical Astronomy Observatories, P.O. Box 26732, Tucson, AZ 85726-6732, USA. [2]Theoretical Astrophysics Center, Danish National Research Foundation, and Institute of Physics and Astronomy, Aarhus University, DK-8000 Aarhus C, Denmark. [3]Hansen Experimental Physics Laboratory, HEPL Annex, Stanford University, Stanford, CA 94305-4085, USA. [4]Astronomy Unit, Queen Mary & Westfield College, University of London, Mile End Road, London E1 4NS, UK. [5]JILA and the Department of Astrophysical and Planetary Sciences, University of Colorado, Boulder, CO 80309-0440, USA.

We have detected changes in the rotation of the sun near the base of its convective envelope, including a prominent variation with a period of 1.3 y at low latitudes. Such helioseismic probing of the deep solar interior has been enabled by nearly continuous observation of its oscillation modes with two complementary experiments. Inversion of the global-mode frequency splittings reveals that the largest temporal changes in the angular velocity Ω are of order 6 nHz, and occur above and below the tachocline that separates the sun's differentially–rotating convection zone (outer 30% by radius) from the nearly uniformly–rotating deeper radiative interior beneath. Such changes are most pronounced near the equator and at high latitudes, and are a substantial fraction of the average 30 nHz difference in Ω with radius across the tachocline at the equator. The results indicate variations of rotation close to the presumed site of the solar dynamo which may generate the 22-year cycles of magnetic activity.

The differential rotation of the sun and its ability to generate large-scale magnetic fields through cyclic dynamo action appear to be intimately linked. It is thought that the global dynamo behavior *(1)* responsible for the emergence of large active regions (sunspot

groups) is derived from strong organized toroidal magnetic fields generated by rotational shear in a thin region, called the tachocline, at the base of the convection zone. The evolving magnetic field could well have a feedback effect on the fluid motion in that region. We are thus motivated to use helioseismology to look for changes in rotation profiles near the tachocline as the sun's magnetic cycle progresses. Here we present evidence that the rotation rate in the interior changes with time, with unexpected periods of about 1.3 y near the equator and possibly 1.0 y at high latitudes.

Helioseismology provides the means to probe the interior structure and dynamics of the sun, using precise observations of the modes of oscillation *(2)*. In particular, the splitting of the global oscillation frequencies by large-scale flows has successfully been used to investigate how the sun's rotation varies with radius and latitude throughout much of the solar interior *(3)*. It was thus found that the angular velocity observed near the solar surface, where the rotation is faster at the equator than near the poles, extends through much of the convection zone (occupying the outer 30% by radius, namely 200 Mm) with little radial dependence. The tachocline *(4, 5)* is a region of strong shear at the base of the convection zone where the angular velocity adjusts to apparent solid-body rotation in the deeper radiative interior (Fig. 1). There is also a thin shear boundary layer near the surface (about 5% by radius or 35 Mm in depth) in which rotation increases with depth at intermediate and low latitudes.

Study of the evolution of such dynamical structures deep within the sun has now become feasible using the nearly continuous full-disk Doppler observations of the sun provided by two independent but complementary helioseismic studies *(6)*, namely the Global Oscillation Network Group (GONG) project involving six ground-based observatories and the Michelson Doppler Imager (MDI) instrument aboard the SOHO spacecraft. The basic data for the analyses are frequency splittings resulting from solar rotation for a broad range of f- and p-mode oscillations *(2)* derived over a 4.5 y time span (from May 1995 to November 1999). These are represented in terms of polynomial expansions in the azimuthal order of the modes; the coefficients in these expansions (the so-called a coefficients) depend on the radial order and degree of the modes. The data from the GONG network were obtained

as 41 overlapping 108-day sets with starting points separated by 36 days, whereas the MDI data consisted of 16 non-overlapping 72-day sets *(7)*. There is considerable temporal overlap, although the GONG observations began earlier, and MDI had a data gap while control of SOHO was temporarily lost. The odd a coefficients were inverted by two different techniques *(8)*, subtractive optimally localized averaging (OLA) and regularized least squares fitting (RLS), to infer the angular velocity Ω as a function of distance r from the solar center and latitude θ. For each experiment (i.e. a given choice of dataset – either GONG or MDI – and inversion method) we calculated an average rotation profile over all the time periods, and subtracted this temporal average (Fig. 1) from the individual profiles. The resulting residuals $\delta\Omega(r,\theta;t)$ (t representing the epoch of the observations) form the basis for the subsequent investigation.

Variations Near The Tachocline Temporal variations of the residuals $\delta\Omega$ are evident (Fig. 2) at selected (r,θ) points using the two independent datasets and the two different inversion methods. The two selected radii $0.72R$ and $0.63R$ (where R is the photospheric radius) lie just above and below the tachocline [which is centered at $0.69R$, as in *(5)*]; the former is near the base of the convection zone and the latter is in the radiative interior. The residuals close to the equator show distinct oscillations with a period of around 1.3 y at both radii. The clearest signal of an oscillatory flow is in the equatorial plane at the radius $0.72R$ (Fig. 2A), having a peak-to-peak variation of about 6 nHz, and in the companion deeper site at $0.63R$ (Fig. 2D) where the phase of the signal is reversed. A smaller-amplitude signal is seen at these depths at 30° latitude (Fig. 2B, 2E). Variations are also visible at the higher latitude of 60°, where the overall variation has increased to about 12 nHz (Fig. 2C), but the signal is more complex. The two sets of observations track well together, and there is good agreement between the two inversion techniques *(9)*. This lends credence to the physical reality of the variations.

Although the variations in $\delta\Omega$ are not strictly periodic, we can estimate the mean period at a given location by sinewave fitting (Fig. 3, 4). The variation of power with frequency (Fig. 3B) at $0.72R$ at the equator peaks at 0.8 y^{-1}, corresponding to a period of 1.3 y; the signal reconstructed from only that frequency is superposed on the data in

Fig. 3A. This single period appears to capture much of the variation in $\delta\Omega$, although the data interval encompasses only about three cycles. Furthermore, analysis of power at that frequency with latitude (Fig. 3C) and with radius (Fig. 3D) reveals that the response is confined to low latitudes and peaks at radii $0.72R$ and $0.63R$. At $0.63R$ the equatorial $\delta\Omega$ signal at that frequency is nearly anti-correlated with the signal at $0.72R$. These results are supported by the other experiments *(10)*. A corresponding sinewave fit of $\delta\Omega$ for latitude 60° and radius $0.72R$ (Fig. 2C) is illustrated in Fig. 4. The variations there are more complex, showing multiple peaks in power (Fig. 4B), with the largest at frequency 1.0 y^{-1} (a period of 1.0 y). We place less significance *(10)* on this identification because of the noisier and more complicated signal, but clearly there is a strong signal (Fig. 4A) that is confined to the higher latitudes (Fig. 4C) and to the base of the convection zone (Fig. 4D). Unlike at lower latitudes, it is more difficult to characterize these variations in terms of a single frequency. However, the correspondence between GONG and MDI in the large excursions, particularly from early 1998 onward, is striking. The significance of the fit in Fig. 3B is substantially reduced at a period 1.0 y compared with 1.3 y (the power is lower at period 1.0 y by a factor of four) so it is improbable that the variations detected at the equator are a product of systematic annual changes in observing conditions or of the orbit of SOHO. Furthermore, although the variations illustrated in Fig. 4 do have a dominant period of 1.0 y, the signal at this period is apparent only near $0.72R$ and 60° (Figs. 4C, 4D), which again argues against the variations being caused by annual systematic observational errors.

We need to assess whether our inferences of changes in $\delta\Omega$ at differing depths and latitudes are genuinely independent measurements, or whether they might be artifacts of the inversion procedure. Two issues are of concern: (i) the finite resolution of the inversions, and (ii) the correlation between the errors in the solutions at different locations. If these were significant, then a signal (either genuine or a result of data errors) at $0.72R$ at the equator could bleed into the inferred solution at other locations. The finite resolution of the inversions causes a genuine signal at one location to be perceived also at other locations. A quantitative measure of this effect is provided by the averaging kernels: the inferred solution at a given location is, apart from errors, an average of the true solution weighted by the

averaging kernel. An example of such an averaging kernel, showing how the solution at radius $0.72R$ on the equator is a weighted average of the rotation over a range of radii and latitudes, is shown in Fig. 5A. Averaging kernels at nearby radii and latitudes are similar. Since the resolution kernels in the region of interest are localized, with weights that are generally positive, resolution issues cannot account for the anti-correlation between the oscillations at $0.72R$ and $0.63R$ on the equator. Error correlation between different points is a more serious concern: the inversions at different locations are based on the same observational data, so the effects of data noise on the inferences at different locations are correlated. Examination of the error correlation functions (Fig. 5B, 5D) shows that the error correlation between $0.72R$ and $0.63R$ at the equator is indeed negative but its magnitude is only about 0.2 for OLA inversion of MDI data, and around 0.4 for the other combinations. Thus we infer that it is unlikely that error correlation accounts for the anti-correlated temporal variations apparent at these locations.

Inversions of global modes are sensitive only to that component of rotation which is symmetrical around the equator *(3)*. Thus the signals illustrated at 30° and 60° latitude are in fact the symmetrized components of the true variations in the sun. If the latter have a substantial antisymmetrical component, which is possible, then the actual fluctuations might be larger than those inferred here.

Physical Implications The detection of substantial variations in rotation rate in the vicinity of the tachocline is of particular interest because this region of strong radial shear is thought to play a crucial role in the cyclic generation of magnetic fields. The overall variations of 6 to 12 nHz in $\delta\Omega$ found at low and high latitudes represent significant signals when compared to the change of 30 to 55 nHz (Fig. 1) in Ω across the tachocline (which varies with latitude in magnitude and in the sign of the rotation gradient).

The oppositely signed tachocline shear at low and high latitudes has a pivotal influence on the mean-field interface dynamos *(1)* currently being considered. These dynamo models seek to provide explanations for the orderly aspects of cyclic variation of the large-scale magnetic activity, involving sunspot eruptions with well-defined rules for field parity

and emergence latitudes. Such highly parameterized models of magnetized turbulent flow within the tachocline have not yet provided detailed predictions of changes in Ω that may be associated with field production as the cycle advances. On the other hand, the latest three-dimensional simulations of turbulent convection in rotating spherical shells *(11)* have made progress in explaining aspects of the differential rotation within the convection zone. However, such global modelling has not yet been able to deal effectively with the intense shear and the highly stable stratification of the tachocline, and therefore is unable to provide reliable estimates of dynamical variations in Ω expected within a zone of rotationally influenced penetrative convection.

The dynamical implications of our detection of $\delta\Omega$ variations are therefore difficult to assess, for the necessary theoretical framework for understanding the tachocline is still at an early stage. However, several dominant properties stand out from our helioseismic inferences. For one, the detected time-varying flows appear to extend at least to $0.63R$, well inside the radiatively stable region. This suggests a strong dynamical coupling between the convection zone and the upper part of the radiative region *(5)*. Further, the anti-correlation of $\delta\Omega$ between radii $0.72R$ and $0.63R$ at low latitudes suggests that angular momentum may be exchanged across the tachocline. The fact that the variation is quasi-periodic is suggestive of a back-and-forth exchange of momentum. The poloidal component of the magnetic field presumed to be present near the base of the convection zone may be the agent responsible for this, as it tends to oppose gradients in angular velocity along field lines. The Alfvén time scale for transport of angular momentum may thus set the periods observed in the variations, though there is considerable uncertainty in the intensity and geometry of the magnetic field close to the tachocline. Another dominant feature of the helioseismic inferences is that variations in $\delta\Omega$ are also clearly present at high latitudes, but these are more erratic in character. There may also be some latitudinal angular-momentum exchange, although this is may be weaker in view of the difference in the dominant periods of oscillation. In any case, the larger variations in $\delta\Omega$ at higher latitudes may reflect the lesser moment of inertia.

Our detection of temporal variations $\delta\Omega$ near the base of the convection zone calls for a continuation of helioseismic data as the solar cycle progresses. Our identification of a

probable period of 1.3 y at low latitudes is tentative, for the data now available extend over less than four such cycles. We need to determine whether these are real periods or aperiodic wobbles, and if are they present in the rising and waning phases of solar activity. We also need to know what relation these variations deep in the sun have to the weak bands of zonal flow detected within the outer 8% of the sun *(12)*, which like the bands of magnetic activity, appear at high latitudes and migrate towards the equator as the cycle proceeds.

The relatively strong $\delta\Omega$ variations at a radius of $0.63R$ at the equator indicates that the radiative interior is more dynamic than might otherwise have been expected. Although the details of the motion in this region, apart from the oscillatory signal found here, are as yet unclear, they may involve weak vertical transport. Such transport would affect the chemical composition of the region beneath the convection zone. Interestingly, helioseismic inversion for solar structure has revealed a sound-speed difference in this region which can plausibly be interpreted as a result of partial mixing which partly counteracts the tendency for helium to settle beneath the convection zone *(13)*. Additional evidence for mixing comes from the depletion of the photospheric lithium abundance by a factor of around 100, relative to the meteoritic abundance (14): nuclear destruction of lithium requires temperatures about 20% higher than the temperature at the convection-zone base in models of the present sun. Taking into account details of the mixing and the change with solar evolution in the depth of the convection zone, mixing in the present sun must extend to a radius of about $0.64R$ *(15)*. Although the depth to which the time-varying flows found here extend into the radiative interior is subject to some uncertainty due to the finite resolution of the inversions, the near coincidence of the two locations is remarkable. The detected variation of rotation close to the presumed site of the solar dynamo may thus also have bearing on the chemical composition realized within the convection zone.

References and Notes

1. The 22-year solar cycles of global magnetic activity might be described by an interface mean-field dynamo, operating in the tachocline, whose rotational shear can stretch poloidal magnetic field generated by cyclonic turbulence in the convection zone into strong toroidal field at its base [E.N. Parker, *Astrophys. J.* **408**, 707 (1993); N.O. Weiss, in *Lectures on Solar and Planetary Dynamos*, M.R.E. Proctor and A.D. Gilbert, Eds. (Cambridge Univ. Press, Cambridge, 1994), pp. 59–95; S.M. Tobias, *Astron. Astrophys.* **322**, 1007, (1997); P. Charbonneau and K.B. MacGregor, *Astrophys. J.* **486**, 502 (1997)]. Such toroidal field should be susceptible to buoyancy instabilities which lead to portions of the field rising through the convection zone and subsequently erupting into the atmosphere as large-scale magnetic loops [P. Caligari, F. Moreno-Insertis, M. Schüssler, *ibid.* **441**, 886, (1995)].

2. For general reviews on helioseismology, see J. Christensen-Dalsgaard, D.O. Gough, J. Toomre, *Science* **229**, 923 (1985); D.O. Gough and J. Toomre, *Annu. Rev. Astron. Astrophys.* **29**, 627 (1991); J. Christensen-Dalsgaard, W. Däppen, W. A. Dziembowski, J.A. Guzik, in *Variable Stars as Essential Astrophysical Tools*, C. İbanoğlu, Ed. (Kluwer, Dordrecht, 2000), pp. 59–167. A mode of oscillation is characterized by the degree l and azimuthal order m of the spherical harmonic which describes its behavior over the solar surface, and the radial order n which typically measures the number of nodes in the displacement eigenfunction in the radial direction. The modes observed on the sun are typically acoustic modes (pressure or p modes), although in the MDI data surface gravity modes (f modes) are also observed at high degree.

3. Recent helioseismic results on solar rotation are presented by M. J. Thompson *et al.*, *Science* **272**, 1300 (1996); T. Corbard *et al.*, *Astron. Astrophys.* **324**, 298 (1997); J. Schou *et al.*, *Astrophys. J.* **505**, 390 (1998). The splitting of global-mode frequencies by rotation provides the means to sample only the latitudinally symmetric component of the variation of angular velocity Ω.

4. The radial gradients of angular velocity Ω in the tachocline may arise from anisotropic turbulent mixing of angular momentum in the stably stratified boundary layer at the

base of the convection zone. The much stronger transport in the latitudinal direction than in the radial direction serves to circumvent the diffusive spread of latitudinal differential rotation into the deeper interior over long time scales [E.A. Spiegel and J.-P. Zahn, *Astron. Astrophys.* **265**, 106 (1992); J.R. Elliott, *ibid.* **327**, 1222 (1997)]. Other models invoke magnetic fields to enforce solid-body rotation in the radiative interior [D.O. Gough and M.E. McIntyre, *Nature* **394**, 755 (1998)]. Linear instability studies of latitudinal shear combined with toroidal magnetic fields [P.A. Gilman and P.A. Fox, *Astrophys. J.* **510**, 1018 (1999); M. Dikpati and P.A. Gilman, *ibid.* **512**, 417 (1999)] suggest mechanisms for achieving enhanced horizontal turbulent mixing in the tachocline.

5. The nearly adiabatic stratification of the convection zone has been determined to extend to a depth of $0.287R$ below the surface, using helioseismic data, with an uncertainty of $0.003R$ or better [J. Christensen-Dalsgaard, D.O. Gough, M.J. Thompson, *Astrophys. J.* **378**, 413 (1991); S. Basu, H.M. Antia, *Mon. Not. R. Astron. Soc.* **287**, 189 (1997)]. The base of this zone at radius $0.713R$ may be contrasted to helioseismic estimates that place the midpoint of the tachocline at radius $0.692R$, with a thickness estimated to be of order 0.02 to $0.09R$ [A.G. Kosovichev, *Astrophys. J.* **469**, L61 (1996); T. Corbard, G. Berthomieu, J. Provost, P. Morel, *Astron. Astrophys.* **330**, 1149 (1998); J.R. Elliott, D.O. Gough, *Astrophys. J.* **516**, 475 (1999); P. Charbonneau *et al.*, *ibid.*, **527**, 445 (1999)]. Thus the tachocline is largely embedded in a region of very stable stratification.

6. The GONG project is described by J.W. Harvey *et al.*, *Science* **272**, 1284 (1996), and the Solar Oscillation Investigation (SOI), which utilizes the MDI instrument, by P.H. Scherrer *et al.*, *Solar Phys.* **162**, 129 (1995).

7. The a coefficients $a_k(n,l)$ used in this study are defined in terms of an expansion of Ω in toroidal vector functions introduced by M.H. Ritzwoller and E.M. Lavely, *Astrophys. J.* **369**, 557 (1991); for a description of the actual implementation used, see J. Schou, J. Christensen-Dalsgaard, M.J. Thompson, *Astrophys. J.* **433**, 389 (1994). The GONG data sets cover the period 1995 May 7 to 1999 Aug 1. Each

set comprises typically 10,000 coefficients, up to a_{15}, for a total of typically 1,200 p-mode multiplets (n,l) for $l \leq 150$. The MDI sets cover the period 1996 May 1 to 1999 November 17, with some interruptions due to problems with the SOHO satellite. These sets contain approximately 30,000 coefficients, up to a_{35}, for roughly 1,800 multiplets with $l \leq 300$. The GONG and MDI data analyses continue to be extended as new observational data become available.

8. In the OLA inversion, linear combinations of the observations are formed such as to correspond to localized averages, in radius and latitude, of the angular velocity, while controlling the error in the inference [F.P. Pijpers and M.J. Thompson, *Astron. Astrophys.* **262**, L33 (1992); see also Schou *et al.* (1998) in *(3)*]. In the RLS technique, a parametrized representation of Ω is fitted to the observations in a least-squares sense, including in the minimization an integral of the square of the second derivative of Ω; this term suppresses the tendency for rapid variations in the solution and also, implicitly, limits the error [Schou *et al.* (1994) in *(7)*]. The methods are controlled by trade-off parameters that provide a balance between resolution and errors. In both cases, the inference can be represented as an average of the true solution, weighted by an averaging kernel whose extent provides a measure of the resolution. In addition to the error, it is important also to take into account the error correlation between the inferences at different locations in the sun [R. Howe and M.J. Thompson, *Mon. Not. R. Astron. Soc.* **281**, 1385 (1996), D.O. Gough, T. Sekii, P. Stark, *Astrophys. J.* **459**, 779 (1996)].

9. The agreement between OLA and RLS inversion methods can be assessed by examining the difference between OLA and RLS rotation residuals $\delta\Omega$ at a given location. As can be seen in Fig. 2, these are within 1-σ in all but a few cases, and the rms of the difference to error ratio for each of the cases illustrated is less than unity.

10. To further quantify the significance of the sinewave fits, we have examined the χ^2 for each fit. For the $(0.72R, 0^\circ)$ case using GONG data and RLS inversion (Fig. 3), the uncertainty in the fitted frequency of $0.78\mathrm{y}^{-1}$ is $\pm 0.01\mathrm{y}^{-1}$, with a reduced χ^2 for the residuals of 0.64. The experiment with GONG data and OLA inversions gives a

frequency of $0.78 \pm 0.01 \mathrm{y}^{-1}$, with reduced χ^2 of 1.16, while combining the GONG and MDI RLS inversions gives a frequency of $0.77 \pm 0.011 \mathrm{y}^{-1}$ with a reduced χ^2 of 0.80. Combining GONG and MDI OLA inversions gives a frequency of $0.77 \pm 0.02 \mathrm{y}^{-1}$ and a reduced χ^2 of 1.26. It is difficult to fit a period to the MDI observations taken alone because of the smaller number of data points and the coarser temporal sampling. For the $(0.72, 60^\circ)$ case (Fig. 4), the GONG data with RLS inversion yields a frequency of $1.01 \pm 0.01 \mathrm{y}^{-1}$ and the reduced χ^2 is 1.32. For combined GONG and MDI RLS inversions the frequency is $1.02 \pm 0.014 \mathrm{y}^{-1}$ and the reduced χ^2 is 1.41. GONG data with OLA inversion gives a frequency of $1.03 \pm 0.005 \mathrm{y}^{-1}$ with a reduced χ^2 of 1.96, and combined GONG and MDI OLA inversions give $1.05 \pm 0.01 \mathrm{y}^{-1}$ with reduced χ^2 of 2.07. The higher χ^2 for all combinations at this location is mostly due to the increase in amplitude later in the period, which is not well reproduced by a single sinewave.

11. Global simulations of turbulent compressible convection in full spherical shells to study the resulting differential rotation have been discussed by J.R. Elliott *et al.*, in *Structure and Dynamics of the Interior of the Sun and Sun-like Stars*, S. Korzennik and A. Wilson, Eds. (ESA SP-418, ESA, Noordwijk, Netherlands, 1998), pp. 765-770; J.R. Elliott, M.S. Miesch, J. Toomre, *Astrophys. J.*, in press (2000); M.S. Miesch *et al.*, *ibid.*, in press (2000).

12. Helioseismic inferences regarding the nature of banded zonal flows in the upper regions of the solar convection zone, and their equatorward migration, are presented by J. Schou *et al.*, in *Proc. IAU Symp. 185: New Eyes to See Inside the Sun and Stars*, F.-L. Deubner, J. Christensen-Dalsgaard, D. W. Kurtz, Eds. (IAU Symp. 185, Kluwer, Dordrecht, 1998), p. 199–212; J. Schou, *Astrophys. J.* **523**, L181 (1999); R. Howe, R. W. Komm, F. Hill, *Solar Phys.*, in press (2000); R. Howe *et al.*, *Astrophys. J. Lett.*, submitted (2000); and J. Toomre *et al.*, *Solar Phys.*, in press (2000). Similar flows on the solar surface had previously been detected through direct Doppler observations [R. Howard and B. J. LaBonte, *Astrophys. J.* **239**, L33 (1980)]. For extensive results of surface observations of these flows, see R.K. Ulrich, in *Structure*

and Dynamics of the Interior of the Sun and Sun-like Stars, S. Korzennik and A. Wilson, Eds. (ESA SP-418, ESA, Noordwijk, Netherlands, 1998), pp. 851–855.

13. A.G. Kosovichev, in *Robotic Exploration Close to the Sun: Scientific Basis*, S.R. Habbal, Ed. (AIP Conf. Proc. 385, Amer. Inst. Phys., Woodbury, NY, 1997), pp. 159–166; M. Takata and H. Shibahashi, *Astrophys. J.* **504**, 1035 (1998); H.M. Antia and S.M. Chitre, *Astron. Astrophys.* **339**, 239 (1998); J.R. Elliott and D.O. Gough, (1999), in *(5)*; A.S. Brun, S. Turck-Chièze, J.-P. Zahn, *Astrophys. J.* **525**, 1032 (1999).

14. E. Anders and N. Grevesse, *Geochim. Cosmochim. Acta* **53**, 197 (1989).

15. As a result of the averaging over the mixed region and over solar evolution, the mean rate of lithium destruction is roughly half the rate at the base of the mixed region in the present sun [J. Christensen-Dalsgaard, D.O. Gough, M.J. Thompson, *Astron. Astrophys.* **264**, 518 (1992)]. Therefore the mixed region needs to extend to a temperature of about 2.76×10^6 K, corresponding to $r \simeq 0.64R$. The precise depth of mixing depends somewhat on the properties of the model.

This work utilizes data obtained by the GONG project, managed by the National Solar Observatory, a Division of the National Optical Astronomy Observatories, which is operated by AURA, Inc. under a cooperative agreement with NSF. The data were acquired by instruments operated by the Big Bear Solar Observatory, High Altitude Observatory, Learmonth Solar Observatory, Udaipur Solar Observatory, Instituto de Astrofísico de Canarias, and Cerro Tololo Interamerican Observatory. The Solar Oscillations Investigation (SOI) involving MDI is supported by NASA grant NAG 5-3077 to Stanford University. SOHO is a mission of international cooperation between ESA and NASA. RWK, and RH in part, were supported by NASA contract S-92698-F. JC-D was supported in part by the Danish National Research Foundation through the establishment of the Theoretical Astrophysics Center. MJT was supported in part by the UK Particle Physics & Astronomy Research Council. JT was supported in part by NASA through grants NAG 5-7996 and NAG 5-8133, and

by NSF through grant ATM-9731676. We thank D. O. Gough for helpful comments on the manuscript.

Figures and Captions

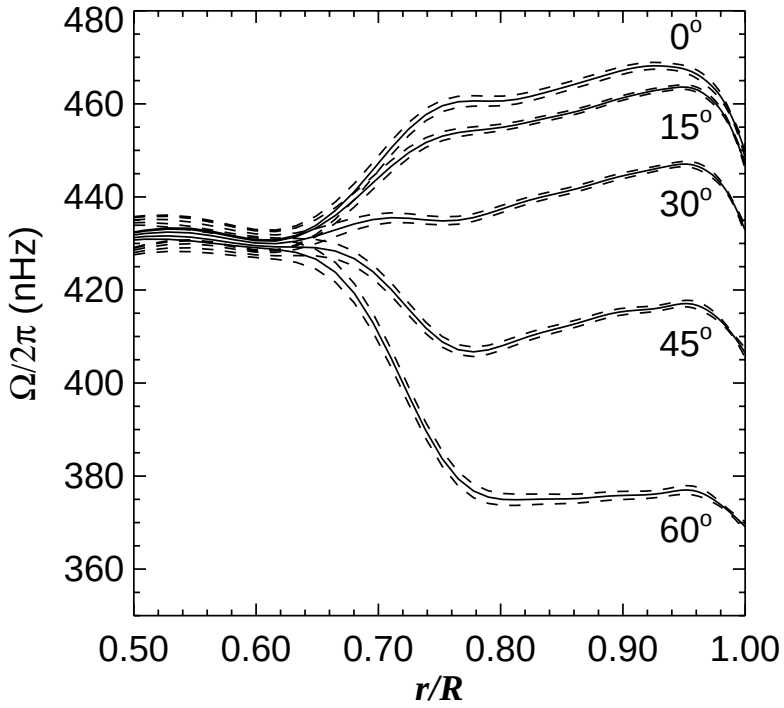

Fig. 1. Time averaged rotation rates $\Omega/2\pi$ obtained from RLS inversion of GONG frequency splittings, plotted against radius at different latitudes. The tachocline is evident near the base of the convection zone, which is determined to be at a radius of $0.713R$ *(5)*. Dashed lines represent 1-σ error bounds for a single inversion.

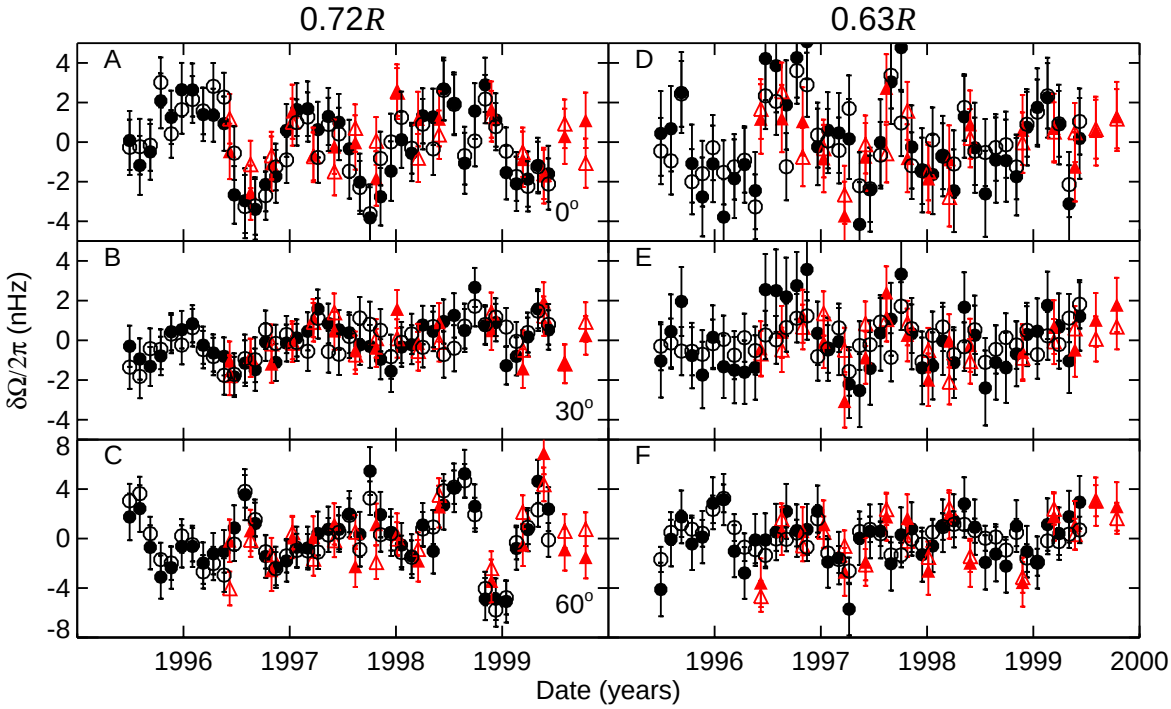

Fig. 2. Variation with time of the residuals $\delta\Omega/2\pi$ in rotation rate at radius $0.72R$, for the three latitudes of (A) 0° (equator), (B) 30°, (C) 60°, and similarly for radius $0.63R$, (D) 0°, (E) 30°, (F) 60°. The symbols denote the data-inversion pairings: GONG–RLS (filled circles, black), GONG–OLA (open circles, black), MDI–RLS (filled triangles, red) and MDI–OLA (open triangles, red).

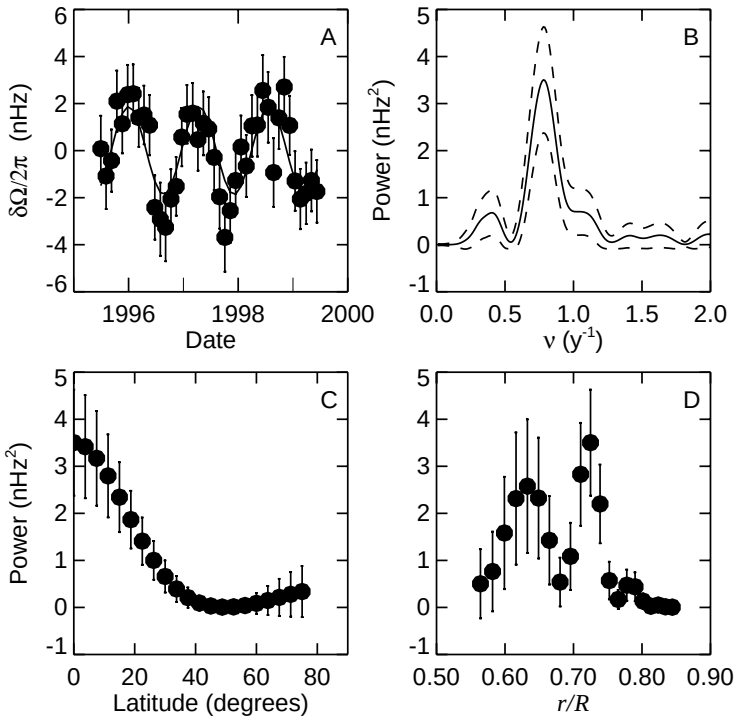

Fig. 3. Sinewave fitting in time of residuals $\delta\Omega/2\pi$ in rotation rate at the equator determined from RLS inversion of GONG data. For each frequency ν, a single sinewave of variable phase $[y = a_1 \cos(2\pi\nu t) + a_2 \sin(2\pi\nu t)]$ was fitted to the time series. (A) Variation at equator of $\delta\Omega/2\pi$ at radius $0.72R$, showing the best-fit sinusoid ($0.78\mathrm{y}^{-1}$) as a solid curve. (B) Power spectrum $[a_1^2 + a_2^2]$ of sinewave fits; dashed lines show 1-σ error bounds. (C) Power at 0.78 y^{-1} frequency as a function of latitude at $0.72R$. (D) Power at same frequency as a function of radius at the equator.

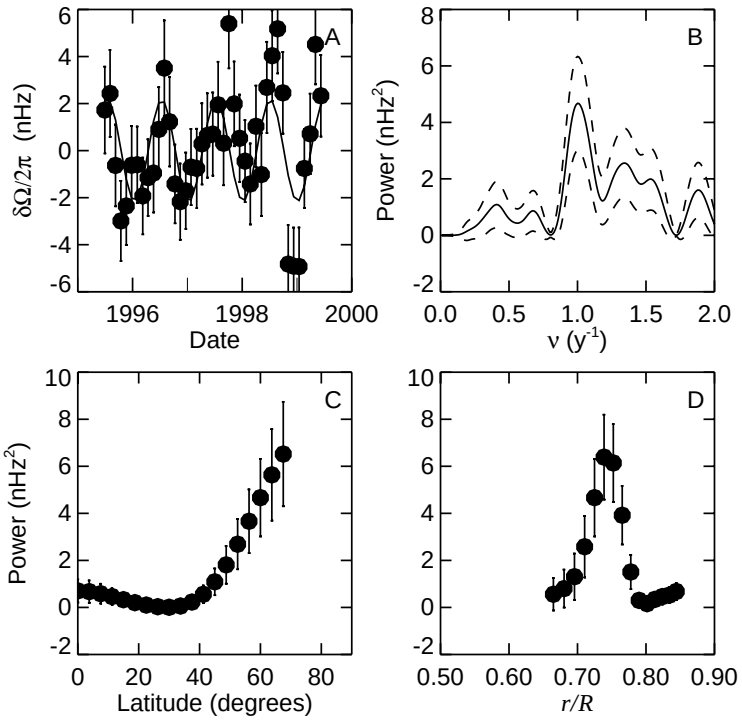

Fig. 4. Sinewave fitting results at latitude of 60° for RLS inversion of GONG data. The notation is the same as in Fig. 3; the dominant frequency is 1.00 y^{-1}.

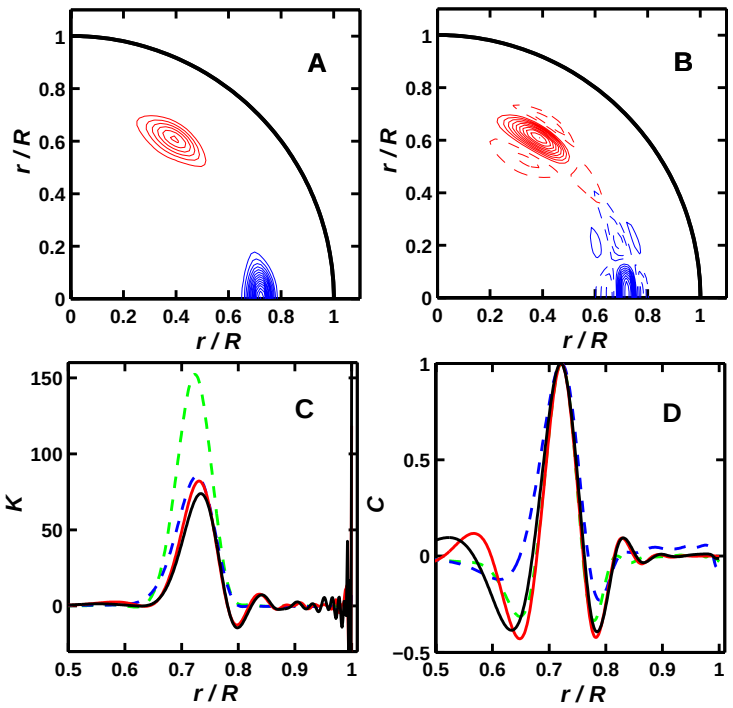

Fig. 5. (A) Contours of the averaging kernels $\mathcal{K}$ and (B) the normalized error-correlation functions $\mathcal{C}$, for OLA inversions of MDI data with target position at radius $0.72R$ at both latitudes $0°$ (blue) and $60°$ (red). The equator is the horizontal axis and the pole the vertical axis. (C) Equatorial cuts through averaging kernels $\mathcal{K}$ for solutions targeted at the equator and $0.72R$ for different pairings of dataset (MDI or GONG) and inversion method (OLA or RLS): shown are MDI–RLS (solid red), MDI–OLA (green dashed), GONG–RLS (solid black), and GONG–OLA (blue dashed). (D) Equatorial cuts through the normalized error-correlation functions $\mathcal{C}$ for the same solution; the line styles are as in (C).